J. Fluid. Mech. (1988), *vol.* 190, *pp.* 39–54
Printed in Great Britain

Nonlinear spiral waves in rotating pipe flow

By N. TOPLOSKY† AND T. R. AKYLAS
Department of Mechanical Engineering, Massachusetts Institute of Technology, Cambridge, Massachusetts 02139

(Received 24 March 1987 and in revised form 30 August 1987)

A numerical investigation of finite-amplitude, non-axisymmetric disturbances, in the form of travelling spiral waves, is made in pipe flow with superimposed solid-body rotation. Rotating pipe flow is found to be supercritically unstable both in the rapid and slow-rotation regimes. Earlier weakly nonlinear calculations, suggesting subcritical instability in the slow-rotation limit, are shown to be in error. Bifurcating neutral waves are calculated for various axial and azimuthal Reynolds numbers and wavenumbers. For fixed axial mean pressure gradient, the axial mean flow induced by these waves gives rise to a significant flux defect, in certain cases as large as 40–50% of the undisturbed mass flux; the possible relevance of this finding to the phenomenon of vortex breakdown is pointed out. In non-rotating pipe flow, no neutral disturbances in the assumed form of spiral waves are found for moderate Reynolds numbers; this indicates that previous conjectures, regarding a possible connection between nonlinear spiral waves in slowly rotating pipe flow and the asymptotic neutral states of Smith & Bodonyi (1982) in non-rotating pipe flow, are not valid.

1. Introduction

It is now recognized that the linear stability properties of fully developed laminar flow in a circular pipe, subjected to rigid rotation about its axis, are markedly different from those of non-rotating pipe flow. Although, in the absence of rotation, pipe flow is entirely stable to infinitesimal perturbations, a relatively minute amount of rigid rotation is capable of causing linear instability (Mackrodt 1976; Cotton & Salwen 1981). Also, in the rapid-rotation regime, Pedley (1969) first showed that rigid rotation has a strong destabilizing effect, giving rise to linear instability at axial Reynolds numbers as low as 83. These theoretical predictions, which inituitively are somewhat surprising given that pipe flow and solid-body rotation by themselves are linearly stable flows, have been confirmed experimentally to a limited extent (Mackrodt 1976; Nagib *et al.* 1971).

Our interest in the stability of rotating pipe flow was originally aroused by the rather unusual behaviour of this flow in the slow-rotation limit and by its possible connection to the instability of non-rotating pipe flow, which at present remains a theoretically unresolved problem. Experimentally, non-rotating pipe flow undergoes transition at a finite Reynolds number greater than about 2100 depending on the particular experimental conditions (Leite 1959; Fox, Lessen & Bhat 1968), while, as remarked earlier, linear stability theory gives no evidence of instability. Furthermore, despite several attempts (Davey & Nguyen 1971; Itoh 1977; Davey 1978*a*; Patera & Orszag 1981), no relevant nonlinear instability mechanism has been

† Present address: Naval Underwater Systems Center, New London, CT 06320, USA.

identified, with the exception of the asymptotic theory of Smith & Bodonyi (1982). Using a nonlinear-critical-layer formalism, valid for large Reynolds numbers, Smith & Bodonyi (1982) were able to find finite-amplitude, neutral, non-axisymmetric modes in the form of spiral waves. It appears that this class of waves exists only for azimuthal wavenumber equal to 1 and their phase speed and axial wavenumber are amplitude-dependent; in particular, as the amplitude decreases, the Reynolds number being large, the axial wavenumber tends to zero and the phase speed approaches a constant value. Interestingly enough, in slowly rotating pipe flow, linear instability also shows up at high axial Reynolds number, for spiral waves with azimuthal wavenumber equal to 1 and axial wavenumber approaching zero as the axial Reynolds number tends to infinity (Mackrodt 1976; Cotton & Salwen 1981). This suggests that perhaps one could reach the class of finite-amplitude modes of Smith & Bodonyi (1982) as the pipe rotation is reduced to zero, by continuation along the branch of finite-amplitude neutral states that bifurcates from linear instability of slowly rotating pipe flow. This speculation was put forward by Akylas & Demurger (1984). Independently, Cowley & Smith (1985) had a similar idea; but, rather than using slowly rotating pipe flow as a starting point of the continuation procedure, they proposed to use flow in a pipe of slightly elliptical cross-section which is also unstable according to linear theory (Davey 1978*b*). Furthermore, through a weakly nonlinear analysis, Akylas & Demurger (1984) found subcritical instability in slowly rotating pipe flow, indicating that finite-amplitude, neutral spiral waves exist for rotation slower than that required for linear instability. Of course, the validity of weakly nonlinear theory is limited to small-amplitude disturbances, close to critical conditions for linear instability; in order to explore the behaviour of nonlinear disturbances as the rotation is reduced to zero, and thereby examine the soundness of the above conjecture, a numerical investigation is required.

Numerical computation of finite-amplitude travelling waves has proven a fruitful approach to the nonlinear stability of certain shear flows. The majority of the existing work has been confined to computations of two-dimensional disturbances on plane shear flows such as plane Poiseuille flow (Zahn *et al.* 1974; Herbert 1976), plane Poiseuille–Couette flow (Herbert 1977; Milinazzo & Saffman 1985) and, more recently, boundary-layer flows (Milinazzo & Saffman 1985). However, as explained earlier, the problem at hand calls for the computation of non-axisymmetric travelling waves in cylindrical geometry. For this purpose, we use an extension of the spectral method proposed by Leonard & Wray (1982), which expands the velocity components in terms of a complete set of divergence-free functions that automatically satisfy the no-slip conditions at the wall of the pipe. The technique was originally tested by Leonard & Wray (1982), who re-obtained the least damped linear mode of non-rotating pipe flow through a time-dependent calculation. Here we present an extension that is particularly suited for computing nonlinear steady disturbances in rotating pipe flow.

As already indicated, the present study was originally motivated by the instability of rotating pipe flow in the slow-rotation limit. However, nonlinear spiral waves are also of some interest in the rapid-rotation regime: the linear spiral instability waves, found by Pedley (1969) in rapidly rotating pipe flow, twist in the opposite direction to the swirl of the basic flow, which makes them possible candidates for explaining the generation of similar backwards spiral disturbances often observed in vortex breakdown (Hall 1972; Leibovich 1978). This proposal, which was first made by Ludwieg (1962, 1965), received some criticism from Hall (1972) and others: it is not clear how weak spiral disturbances, arising from a linear instability mechanism, can

lead to the dramatic flow changes, in particular axial-flow stagnation, that accompany vortex breakdown. In this respect, the changes induced in the basic flow by the presence of finite-amplitude spiral waves could provide some useful information about the possible relevance of the instability mechanism proposed by Ludwieg to the phenomenon of vortex breakdown.

2. Formulation

Consider fully developed laminar flow in an infinitely long, circular pipe of radius r_o, $0 \leqslant r \leqslant r_o$, $-\infty < z < \infty$, subjected to rigid rotation about its axis with constant angular velocity ω. The basic steady flow, which is driven by a constant axial pressure gradient, is the combination of a parabolic velocity profile, $W_0(1-r^2/r_0^2)$, with centreline velocity W_0 in the axial direction, and solid-body rotation, ωr, in the azimuthal direction. Our interest centres on finite-amplitude perturbations to this basic flow in the form of periodic spiral waves travelling with constant phase speed. Taking the axial wavelength to be $2\pi L$, three relevant dimensionless parameters are the axial Reynolds number R, the azimuthal Reynolds number Ω, and the dimensionless axial wavenumber μ:

$$R = \frac{W_0 r_0}{\nu}, \quad \Omega = \frac{\omega r_0^2}{\nu}, \quad \mu = \frac{r_0}{L}, \tag{1}$$

where ν is the fluid kinematic viscosity. Earlier work (Mackdrodt 1976) has shown that, in terms of these parameters, the slow-rotation regime (in which we seek the least amount of rotation needed to linearly destabilize a primarily axial flow) is defined by the limit

$$\Omega = O(1), \quad \tilde{R} = \mu R = O(1), \quad \mu \to 0. \tag{2}$$

On the other hand, the rapid-rotation regime (in which we seek the least amount of axial flow needed to linearly destabilize a predominantly azimuthal flow) is realized in the limit (Pedley 1969)

$$R = O(1), \quad \tilde{\Omega} = \mu\Omega = O(1), \quad \mu \to 0. \tag{3}$$

The appropriate scalings of the perturbation-velocity components and pressure differ in these two extremes; we choose to scale according to the slow-rotation regime but, as will be discussed later (see §4), this choice does not prohibit us from studying the rapid-rotation regime as well. Thus, we define dimensionless (primed) variables according to

$$r = r_0 r', \quad z = Lz', \quad t = \frac{L}{W_0}t', \quad (u, v) = \mu W_0(u', v'), \quad w = W_0 w', \quad p = \mu^2 \rho W_0^2 p', \tag{4}$$

where t is time, $\boldsymbol{u} = (u, v, w)$ are the radial, azimuthal and axial perturbation-velocity components in cylindrical coordinates (r, θ, z), p is the perturbation pressure, and ρ is the fluid density. Dropping the primes, the governing equations in dimensionless form are

$$\frac{\partial \boldsymbol{u}}{\partial t} + \mathbf{L}\boldsymbol{u} + \boldsymbol{\nabla}_\mu p - \frac{1}{\tilde{R}}\nabla_\mu^2 \boldsymbol{u} + \boldsymbol{N} = 0, \tag{5}$$

$$\boldsymbol{\nabla}\cdot\boldsymbol{u} = 0, \tag{6}$$

where
$$\mathbf{L} \equiv \begin{bmatrix} \mathrm{D} & -2\Omega/\tilde{R} & 0 \\ 2\Omega/\tilde{R} & \mathrm{D} & 0 \\ -2r & 0 & \mathrm{D} \end{bmatrix}, \tag{7a}$$

with
$$\mathrm{D} \equiv \frac{\Omega}{\tilde{R}} \frac{\partial}{\partial \theta} + (1-r^2) \frac{\partial}{\partial z}, \tag{7b}$$

$$\boldsymbol{N} = \begin{Bmatrix} uu_r + vu_\theta/r + wu_z - v^2/r \\ uv_r + vv_\theta/r + wv_z + uv/r \\ uw_r + vw_\theta/r + ww_z \end{Bmatrix}, \tag{8}$$

$$\nabla_\mu^2 \boldsymbol{u} = \begin{Bmatrix} \nabla_\mu^2 u - u/r^2 - 2v_\theta/r^2 \\ \nabla_\mu^2 v - v/r^2 + 2u_\theta/r^2 \\ \nabla_\mu^2 w \end{Bmatrix} \tag{9a}$$

with
$$\nabla_\mu^2 \equiv \frac{1}{r} \frac{\partial}{\partial r} \left(r \frac{\partial}{\partial r} \right) + \frac{1}{r^2} \frac{\partial^2}{\partial \theta^2} + \mu^2 \frac{\partial^2}{\partial z^2}, \tag{9b}$$

and
$$\boldsymbol{\nabla}_\mu \equiv \left\{ \frac{\partial}{\partial r}, \frac{1}{r} \frac{\partial}{\partial \theta}, \mu^2 \frac{\partial}{\partial z} \right\}. \tag{10}$$

Finite-amplitude, periodic spiral-wave solutions of the governing equations (5), (6) can be formally expanded in Fourier series:

$$\boldsymbol{u} = \sum_{k=-\infty}^{\infty} \boldsymbol{u}^k(r)\, \mathrm{e}^{\mathrm{i}k\phi}, \quad p = \sum_{k=-\infty}^{\infty} p^k(r)\, \mathrm{e}^{\mathrm{i}k\phi} \quad (0 \leqslant r \leqslant 1), \tag{11}$$

where
$$\phi = z + l\theta - ct; \tag{12}$$

here l is the (integer) azimuthal wavenumber, c is the constant real phase speed and, in view of the scalings chosen in (4), the axial wavelength is normalized to 2π. Also, since $\boldsymbol{u}$ and p are real,
$$\boldsymbol{u}^{-k} = \boldsymbol{u}^{k*}, \quad p^{-k} = p^{k*}, \tag{13}$$

where * denotes complex conjugate, so that the sums in (11) may be restricted to $k \geqslant 0$. It is worth emphasizing that the spiral waves (11) comprise only a special class of solutions which, for reasons already discussed in §1, are of particular interest here; more complicated non-axisymmetric solutions would require the use of separate Fourier series in the axial and azimuthal directions.

For given values of the parameters R, Ω, μ and the wavenumber l (plus a phase normalization to be discussed in §3), the unknown Fourier coefficients $\boldsymbol{u}^k, p^k$ and the phase speed c are determined by requiring that the series (11) satisfy (5), (6), subject to regularity conditions at the centre ($r = 0$) and the no-slip condition at the wall of the pipe ($r = 1$); this task has to be dealt with numerically and a suitable procedure is outlined in §3. After the solution has been obtained, it is convenient to have a measure of the size of the perturbation and, for this purpose, we choose the relative kinetic energy of the fluctuating harmonics ($|k| \geqslant 1$) in (11), averaged over one axial wavelength:
$$E = \sum_{k=1}^{\infty} E_k, \tag{14}$$

where

$$E_k = \frac{2\pi}{E_b}\int_0^1 r\mathrm{d}r(\mu^2|u^k|^2+\mu^2|v^k|^2+|w^k|^2), \tag{15a}$$

and E_b is the kinetic energy of the basic flow per unit length in the axial direction:

$$E_b = \tfrac{1}{2}\pi\left(\frac{1}{3}+\frac{1}{2}\mu^2\frac{\Omega^2}{\tilde{R}^2}\right). \tag{15b}$$

Similarly, in order to quantify the axial and azimuthal mean-flow components induced by the perturbation disturbance (represented by the $k = 0$ harmonic in (11)), the associated mass flux Φ and Γ, the circulation about the axis averaged over the pipe radius, are defined

$$\Phi = \frac{2\pi}{\Phi_b}\int_0^1 r\mathrm{d}r\, w^0, \quad \Gamma = \frac{2\pi}{\Gamma_b}\int_0^1 r\mathrm{d}r\,\mu v^0, \tag{16a}$$

where Φ_b, Γ_b are the corresponding quantities for the basic flow:

$$\Phi_b = \tfrac{1}{2}\pi, \quad \Gamma_b = \frac{2\pi}{3}\mu\frac{\Omega}{\tilde{R}}. \tag{16b}$$

Note that in this discussion the mean axial pressure gradient driving the flow is kept fixed and, thus, the disturbance is allowed to modify the mass flux of the basic flow; another choice would be to keep the mass flux fixed and allow the pressure gradient to vary. For finite-amplitude perturbations, these two formulations are not equivalent.

3. Numerical method

The numerical procedure for computing spiral-wave solutions of the form (11) follows along the lines of the technique developed by Leonard & Wray (1982). The overall strategy is to expand each velocity Fourier mode $\boldsymbol{u}^k(r)\,\mathrm{e}^{\mathrm{i}k\phi}$ in terms of a complete set of divergence-free vector functions $\{\boldsymbol{\chi}_n^k(r)\,\mathrm{e}^{\mathrm{i}k\phi}\}$, which behave appropriately as $r \to 0$ and satisfy the no-slip condition at $r = 1$:

$$\boldsymbol{u}^k(r) = \sum_n a_n^k \boldsymbol{\chi}_n^k(r), \tag{17}$$

$$\boldsymbol{\nabla}\cdot\boldsymbol{\chi}_n^k(r)\,\mathrm{e}^{\mathrm{i}k\phi} = 0, \quad \boldsymbol{\chi}_n^k(r=1) = 0. \tag{18}$$

The coefficients a_n^k of the spectral expansion (17) are then determined from the momentum equation (5), which is discretized through a weighted-residual technique, using a set of vector weight functions $\{\boldsymbol{\xi}_m^k(r)\,\mathrm{e}^{-\mathrm{i}k\phi}\}$ that are well-behaved at $r = 0$ and satisfy the following requirements:

$$\boldsymbol{\nabla}_\mu\cdot\boldsymbol{\xi}_m^k(r)\,\mathrm{e}^{-\mathrm{i}k\phi} = 0, \quad \boldsymbol{\xi}_m^k(r=1)\cdot\hat{\boldsymbol{e}}_r = 0, \tag{19}$$

$\hat{\boldsymbol{e}}_r$ being the unit vector in the radial direction. To be more specific, inserting the expansions (11), (17) into the momentum equation (5), and taking the inner product with each of the weight functions, leads to an infinite set of algebraic equations for the unknown coefficients a_n^k:

$$\left[\mathrm{i}kc\,A_{mn}^k+\frac{1}{\tilde{R}}B_{mn}^k+\mathrm{i}C_{mn}^k\right]a_n^k+N_m^k = 0, \tag{20}$$

where repeated subscripts are automatically summed (here and throughout this paper) and

$$A^k_{mn} = -\int_0^1 r\,\mathrm{d}r\,\boldsymbol{\chi}^k_n\,\mathrm{e}^{\mathrm{i}k\phi}\cdot\boldsymbol{\xi}^k_m\,\mathrm{e}^{-\mathrm{i}k\phi}, \tag{21a}$$

$$B^k_{mn} = -\int_0^1 r\,\mathrm{d}r\,\nabla^2_\mu\boldsymbol{\chi}^k_n\,\mathrm{e}^{\mathrm{i}k\phi}\cdot\boldsymbol{\xi}^k_m\,\mathrm{e}^{-\mathrm{i}k\phi}, \tag{21b}$$

$$C^k_{mn} = -\mathrm{i}\int_0^1 r\,\mathrm{d}r\,\mathbf{L}\boldsymbol{\chi}^k_n\,\mathrm{e}^{\mathrm{i}k\phi}\cdot\boldsymbol{\xi}^k_m\,\mathrm{e}^{-\mathrm{i}k\phi}, \tag{21c}$$

$$N^k_m = \frac{1}{2\pi}\int_0^{2\pi}\mathrm{d}\phi\int_0^1 r\mathrm{d}r\,\boldsymbol{N}\cdot\boldsymbol{\xi}^k_m\,\mathrm{e}^{-\mathrm{i}k\phi}. \tag{21d}$$

Note that, owing to conditions (19), the pressure term has dropped out of (20); if the pressure field is desired, it can be calculated through the solution of a Poisson equation, after the velocity field has been obtained. Also, each term in (20) has a clear interpretation: the first three terms, which are linear in a^k_n, represent, respectively, the temporal acceleration, the viscous term, and the interaction of the basic flow with the perturbation; the last term, which couples the different Fourier modes, represents the nonlinear perturbation interactions.

The success of the spectral technique depends heavily on the specific choice of expansion and weight functions. With the exception of the $k = 0$ family, we use the same sets of expansion and weight vectors as those proposed by Leonard & Wray (1982). In particular, each set $\{\boldsymbol{\chi}^k_n(r)\}$ is divided into three families, denoted by (-1) (which contains only a single vector), $(+)$, and $(-)$:

$$\{\boldsymbol{\chi}^k_n\} = \{\boldsymbol{\chi}^k_{-1};\boldsymbol{\chi}^{k+}_0,\ldots,\boldsymbol{\chi}^{k+}_n,\ldots;\boldsymbol{\chi}^{k-}_0,\ldots,\boldsymbol{\chi}^{k-}_n,\ldots\} \quad (k\geqslant 0) \tag{22}$$

and $\{\boldsymbol{\chi}^{k\pm}_n\}$ are divided from a generating vector

$$\boldsymbol{\chi}^{k\pm}_n\,\mathrm{e}^{\mathrm{i}k\phi} = \boldsymbol{\nabla}\times\boldsymbol{\alpha}^\pm_n\,\mathrm{e}^{\mathrm{i}k\phi} \quad (k\geqslant 1,\ n\geqslant 0), \tag{23}$$

where
$$\boldsymbol{\alpha}^\pm_n = \{-\mathrm{i}q^\pm_n, \mp q^\pm_n, 0\}, \tag{24a}$$

with
$$q^\pm_n \equiv q^{s\pm1}_n = r^{s\pm1}(1-r^2)^2 g^{s\pm1}_n(r^2), \tag{24b}$$

g^s_n being a shifted Jacobi polynomial (Abramowitz & Stegun 1968, p. 773) and $s = kl$. Also,

$$\boldsymbol{\chi}^k_{-1} = \boldsymbol{\chi}^{k+}_{-1} + \boldsymbol{\chi}^{k-}_{-1} \quad (k\geqslant 1), \tag{25}$$

where $\boldsymbol{\chi}^{k\pm}_{-1}$ are derived from (23), (24a) with $q^\pm_{-1} = r^{s\pm1}(1-r^2)$. The three corresponding families of vector weight functions for each $k\geqslant 0$ are chosen in an analogous fashion:

$$\{\boldsymbol{\xi}^k_m\} = \{\boldsymbol{\xi}^k_{-1};\boldsymbol{\xi}^{k+}_0,\ldots,\boldsymbol{\xi}^{k+}_m,\ldots;\boldsymbol{\xi}^{k-}_0,\ldots,\boldsymbol{\xi}^{k-}_m,\ldots\} \quad (k\geqslant 0), \tag{26}$$

$$\boldsymbol{\xi}^{k\pm}_m\,\mathrm{e}^{-\mathrm{i}k\phi} = \boldsymbol{\nabla}_\mu\times\boldsymbol{\nabla}\times\boldsymbol{\beta}^\pm_m\,\mathrm{e}^{-\mathrm{i}k\phi} \quad (k\geqslant 1,\ m\geqslant 0), \tag{27}$$

where
$$\boldsymbol{\beta}^\pm_m = \{\mathrm{i}q^\pm_m, \mp q^\pm_m, 0\}, \tag{28}$$

and
$$\boldsymbol{\xi}^k_{-1} = \{-\mathrm{i}r^{s+1} + \mathrm{i}r^{s-1}g^{s-1}_1,\ r^{s+1} + r^{s-1}g^{s-1}_1, 0\} \quad (k\geqslant 1). \tag{29}$$

It is straightforward to verify that the above sets of vector functions $\{\boldsymbol{\chi}^k_n(r)\,\mathrm{e}^{\mathrm{i}k\phi}\}$, $\{\boldsymbol{\xi}^k_m(r)\,\mathrm{e}^{-\mathrm{i}k\phi}\}$ behave correctly as $r\to 0$ and fulfil the requirements (18), (19) imposed earlier. Finally, the choice of expansion and weight vector functions for $k = 0$ requires extra care. In view of our earlier assumption of fixed mean axial

pressure gradient, it is clear that the mean flow induced by the perturbation should not generate a mean axial shear stress at $r = 1$. Furthermore, it can be shown (see Appendix) that no mean azimuthal shear stress is present at $r = 1$ either; in other words, the torque required to maintain the constant angular velocity of the pipe vanishes. Accordingly, for $k = 0$, the expansion vectors

$$\chi^0_{-1} = 0, \quad \chi^{0+}_n = \{0, 0, q^0_n\}, \quad \chi^{0-}_n = \{0, q^1_n, 0\} \quad (n \geqslant 0) \tag{30}$$

are used so that the above conditions are automatically met. The corresponding weight functions for $k = 0$ are

$$\xi^0_{-1} = 0, \quad \xi^{0+}_m = \{0, 0, \nabla^2_\mu q^0_m\}, \quad \xi^{0-}_m = \{0, \nabla^2_\mu q^1_m, 0\} \quad (m \geqslant 0). \tag{31}$$

In implementing the spectral technique numerically, the infinite series (11) and (17) are truncated at a finite number of Fourier modes $k = K$ and expansion functions $n = N$, say, with an equal number ($m \leqslant N$) of weight functions. Thus, (20) reduces to a finite set of algebraic equations for a finite number of unknowns. More specifically, for $k = 0$, as there is no (-1) family of expansion and weight functions, equations (20) give $2N+2$ real equations while for $1 \leqslant k \leqslant K, 2K(2N+3)$ real equations are obtained, a total of $(2K+1)(2N+3)-1$ real equations. On the other hand, there are $(2K+1)(2N+3)$ real unknowns, consisting of a^0_n, the real and imaginary parts of a^k_n ($1 \leqslant k \leqslant K$), and the phase speed c. The additional equation is provided by a phase normalization which, in this calculation, is chosen so that the real part of $u^1(r)$ vanishes at some radial point close to $r = 0.5$. Thus, the number of unknowns matches the number of equations, which can now be solved iteratively through a multi-dimensional Newton's method to obtain the velocity field and the phase speed for given values of the parameters R, Ω, μ and l; subsequently, the energy, mass flux and average circulation, associated with a spiral wave, can be readily computed from (14), (15) and (16).

It is remarkable that, although the detailed implementation of the numerical procedure outlined above is quite involved, a number of steps, prior to numerical solution of the final system of nonlinear equations, can be carried out analytically. Leonard & Wray (1982) noted that the matrices with elements A^k_{mn}, B^k_{mn} in (20) are tightly banded and can be evaluated analytically using properties of the shifted Jacobi polynomials (Abramowitz & Stegun 1968, p. 773). It turns out that the matrix with elements C^k_{mn} in (20) is also partially banded (but not as sparse as A^k_{mn}, B^k_{mn}) and can be evaluated analytically (Toplosky 1987); thus all matrix elements of the linear-stability eigenvalue problem are derived from analytic expressions. A major portion of the computational effort is devoted to calculating the nonlinear coupling terms N^k_m in (20) numerically, using the trapezoidal rule; these involve integrals of triple products of shifted Jacobi polynomials and cannot be evaluated exactly. Further details concerning questions of numerical implementation can be found in Toplosky (1987). The different tests used to check the accuracy of the calculations are described below together with the results.

4. Results

As explained in §3, the procedure for computing finite-amplitude neutral spiral waves is iterative and requires a sufficiently accurate initial guess in order to achieve convergence. A convenient point of departure for the iteration is provided by the results of linear and weakly nonlinear theories, close to critical conditions for linear

instability; these known results are also used as partial checks of the numerical technique. In particular, the eigenvalue problem of linear-stability theory, where c is the eigenvalue, is readily obtained from (20) with $k = 1$ and $N_m^k = 0$. Linear-neutral-stability curves (c real) were calculated for various combinations of R, Ω, μ, l, both in the slow and rapid-rotation regimes (2), (3), and complete agreement with results of previous work (Mackrodt 1976; Cotton & Salwen 1981; Pedley 1969) was found; this leads us to believe that the matrix elements A_{mn}^k, B_{mn}^k, C_{mn}^k in (20) were computed correctly. As expected, calculations could not be carried out arbitrarily close to the fast-rotation limit (3) ($\mu = 0$), as the adopted scalings of the velocity components (4) are not valid there; however, for moderately small values of $\mu (0.01 \leqslant \mu \leqslant 0.2)$, which cause no trouble numerically, comparison with the asymptotic results of Pedley (1969) indicates that the fast-rotation limit has essentially been reached and, thus, no rescaling was deemed necessary in order to examine this limit.

In the weakly nonlinear theory, valid close to critical conditions for linear instability, the disturbance amplitude is small and the primary harmonic ($k = 1$) in (11) dominates, so that

$$\boldsymbol{u} = \epsilon(\boldsymbol{u}^{11} \mathrm{e}^{\mathrm{i}\phi} + *) + \epsilon^2 \boldsymbol{u}^{02} + \epsilon^2(\boldsymbol{u}^{22} \mathrm{e}^{2\mathrm{i}\phi} + *) + \epsilon^3(\boldsymbol{u}^{13} \mathrm{e}^{\mathrm{i}\phi} + *) + \ldots, \tag{32}$$

$$c = c_0 + \epsilon^2 c_2 + \ldots, \tag{33}$$

$$\Omega = \Omega_0 + \epsilon^2 \Omega_2 + \ldots, \tag{34}$$

where $\epsilon (\ll 1)$ is a measure of the disturbance amplitude, c_0 and $\boldsymbol{u}^{11}$ are the eigenvalue and eigenfunction, respectively, of linear theory at critical conditions, and $\epsilon^2 c_2$ is the leading-order nonlinear correction to the phase speed; also, it has been assumed that the parameters $\tilde{R}$, μ, l are kept fixed and Ω is perturbed by $\epsilon^2 \Omega_2$ so that c remains real. The mean-flow and second-harmonic corrections $\boldsymbol{u}^{02}$ and $\boldsymbol{u}^{22}$ are directly obtained from (20) with $k = 0$, 2, respectively, since the nonlinear coupling terms N_m^k are known (to this order of approximation) in terms of the primary harmonic. Proceeding to $O(\epsilon^3)$, the nonlinear correction $\boldsymbol{u}^{13} \mathrm{e}^{\mathrm{i}\phi}$ to the primary satisfies an inhomogeneous problem of the form

$$\left[\mathrm{i}c_0 A_{mn}^1 + \frac{1}{\tilde{R}} B_{mn}^1 + \mathrm{i} C_{mn}^1\right] a_n^{13} = -N_m^1 - \mathrm{i}\left[c_2 A_{mn}^1 + \Omega_2 \frac{\partial}{\partial \Omega} C_{mn}^1\right] a_n^{11}, \tag{35}$$

where again N_m^1 is known in terms of $\boldsymbol{u}^{11}$, $\boldsymbol{u}^{02}$ and $\boldsymbol{u}^{22}$. Following the usual orthogonality argument, the above algebraic system has no solution (c_0 is an eigenvalue), unless the right-hand side is orthogonal to the solution of the corresponding homogeneous transpose system:

$$\left[N_m^1 + \mathrm{i}\left(c_2 A_{mn}^1 + \Omega_2 \frac{\partial}{\partial \Omega} C_{mn}^1\right) a_n^{11}\right] a_m^{1t} = 0, \tag{36}$$

where

$$\left[\mathrm{i}c_0 A_{nm}^1 + \frac{1}{\tilde{R}} B_{nm}^1 + \mathrm{i} C_{nm}^1\right] a_n^{1t} = 0. \tag{37}$$

The solvability condition (36), which is equivalent to two real equations, specifies the unknown corrections, c_2 and Ω_2. Also, the Landau constant λ at critical conditions ($\Omega_2 = 0$), as defined by Akylas & Demurger (1984), is given by

$$\lambda = \frac{a_m^{1t} N_m^1}{a_m^{1t} (A_{mn}^1 a_n^{11})}, \tag{38}$$

l	μ	$\tilde{R}$	Ω	Re λ	Im λ
1	0	106.6	−26.96	−35.4	13.9
2	0	165.7	−43.47	−21.2	24.0
1	1	155.8	−33.52	−90.3	55.1
2	1	192.7	−53.54	−31.7	38.7
3	0	232.6	−69.77	−15.0	23.2
1	0.1	8.305	−415.5	−507	−15
2	0.1	9.117	−910.8	−607	20
1	1	109.3	−52.06	−128	57
2	1	107.7	−105.5	−88	38

TABLE 1. Landau constant λ at linear-neutral-stability conditions for various combinations of parameters, l, μ, $\tilde{R}$ and Ω

with the understanding that the normalization of $\boldsymbol{u}^{11}$ is the same as in Akylas & Demurger (1984), namely $rw^{11} = 1$ where $|rw^{11}|$ attains its maximum value in $0 < r < 1$. Comparing the results of weakly nonlinear theory, obtained from the above formulation, with those of Akylas & Demurger (1984) in the slow-rotation limit, it is found that the mean-flow and second-harmonic corrections $\boldsymbol{u}^{02}$, $\boldsymbol{u}^{22}$ are in excellent agreement; however, the corresponding values of the Landau constant λ are at variance. In particular, the present calculations give Re $\lambda < 0$, suggesting supercritical instability, while Akylas & Demurger (1984) find Re $\lambda > 0$, implying subcritical instability. To resolve this conflict, the Landau constant was re-calculated by a different method, using a solvability condition based on the adjoint eigenvalue problem, and the results agreed with the present calculations. Also, going back to the work of Akylas & Demurger (1984), a programming error was discovered in the calculation of the inhomogeneous solution of the $O(\epsilon^3)$ correction to the primary harmonic; when this was corrected, the results of all three methods were consistent. Thus, we feel confident that the values of the Landau constant listed in table 1 are correct.

Using as a starting point the weakly nonlinear results described above, finite-amplitude calculations were carried out by continuation in either $\tilde{R}$ or Ω, keeping the rest of the parameters fixed. Typical plots of the energy of the disturbance (calculated from (14), (15), after the infinite sum in (14) has been truncated at $k = K$) as a function of $\tilde{R}$ and Ω for $l = 1$ are shown in figure 1 (a, b). In particular, figure 1 (a) refers to the slow-rotation limit and figure 1 (b) to the rapid-rotation limit; the corresponding linear-neutral-stability curves are indicated with a dotted line in the $(\tilde{R}, \Omega)$ plane. It is clear that all branches of finite-amplitude spiral waves bifurcate supercritically in both regimes of rotation and there is no sign of appearance of limit points. This was found to be the case for $l = 1$, 2, 3 and all values of μ in the range $0.1 \leqslant \mu \leqslant 1$ examined. For very small values of the disturbance energy, the numerical results agree closely with the predictions of weakly nonlinear theory and this provides an additional check of the calculations.

Turning now to a more quantitative discussion of the nonlinear results, figure 2 (a, b, c) presents plots of the disturbance energy E, induced mass flux Φ, and average circulation Γ, in three particular cases; for convenience, Φ and Γ, which have already been normalized in (16) with respect to the basic flow, are shown in per cent in order to bring out the effect of the disturbance on the unperturbed flow more clearly. Figure 2 (a) refers to the branch that bifurcates from the point of the linear-neutral-stability curve that requires the minimum amount of rotation for linear

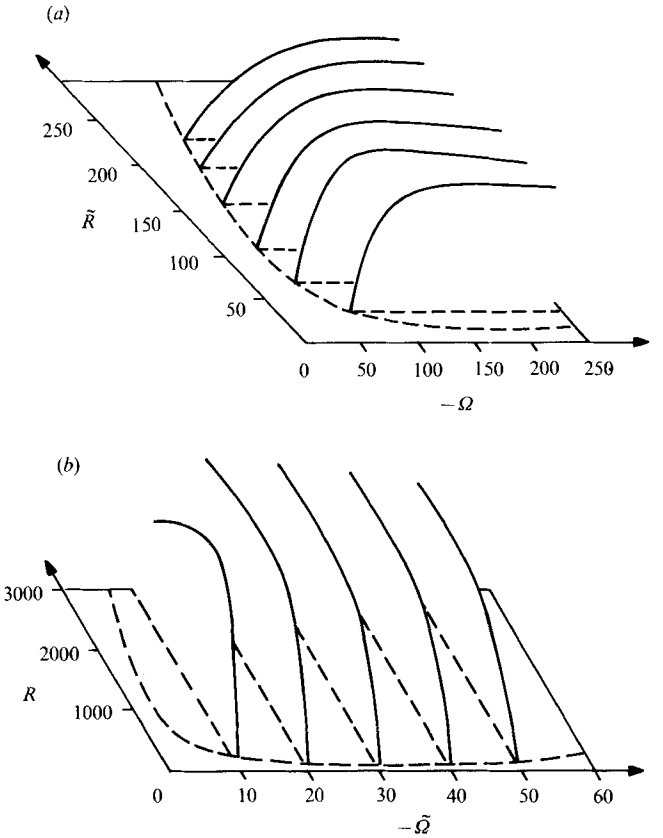

FIGURE 1. Bifurcating branches of finite-amplitude spiral waves as functions of $\tilde{R}$ and Ω. (*a*) slow-rotation regime ($l = 1$, $\mu = 0$; $K = 2$, $N = 8$). (*b*) rapid-rotation regime ($l = 1$, $\mu = 0.1$; $K = 2$, $N = 8$).

instability in the slow-rotation limit ($\Omega = -26.96$, $\tilde{R} = 106.6$, $l = 1$, $\mu = 0$). As the rotation is increased (in absolute value) beyond $\Omega = -26.96$ for fixed $\tilde{R} = 106.6$, the induced mass flux Φ, which is always negative implying a mass-flux defect, rises significantly and reaches a value close to 30% of the undisturbed flux; this is in contrast to the induced average circulation, which always remains less than 10% of the undisturbed value and is positive, again indicating a circulation defect (since $\Omega < 0$). Figure 2(*b*) displays the branch that bifurcates from the point that requires the minimum amount of axial flow for linear instability in the rapid-rotation regime ($R = 83.05$, $\tilde{\Omega} = -41.55$, $l = 1$, $\mu = 0.1$). As R is increased past critical, for fixed $\tilde{\Omega}$, the induced mass flux Φ, which is again a flux defect, rises very steeply compared with the disturbance energy and reaches a maximum of about 30% of the basic flux; the induced circulation is again relatively small. A similar situation is shown in figure 2(*c*) for the branch that bifurcates from $R = 91.17$, $\tilde{\Omega} = -91.08$ for $\mu = 0.1$, $l = 2$; however, here as R is increased, keeping the rest of the parameters fixed, the induced flux defect reaches a value close to 50%, while the disturbance energy and induced circulation still remain relatively very small.

The results reported above were obtained after having truncated the Fourier series (11) at a finite number of Fourier modes ($0 \leqslant k \leqslant K$) and the spectral expansion (17) at a finite number of expansion vectors ($n \leqslant N$). The effect of this truncation on the

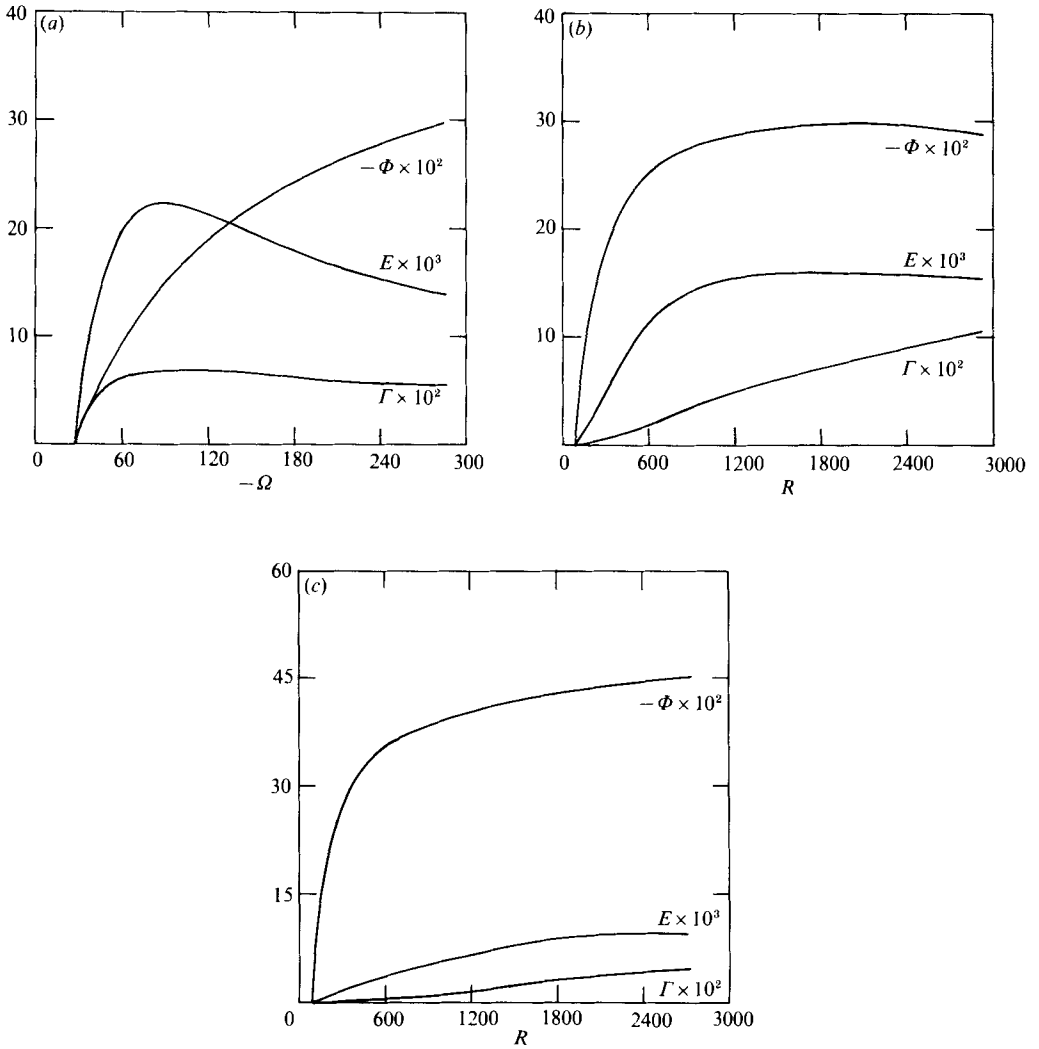

FIGURE 2. Disturbance energy E, induced flux Φ, and average circulation Γ. (*a*) slow-rotation regime; $\tilde{R} = 106.6$ and Ω is increased past bifurcation point at $\Omega = -26.96$ ($l = 1$, $\mu = 0$; $K = 4$, $N = 10$). (*b*) rapid-rotation regime; $\tilde{\Omega} = -41.55$ and R is increased past bifurcation point at $R = 83.05$ ($l = 1$, $\mu = 0.1$; $K = 4$, $N = 10$). (*c*) rapid-rotation regime; $\tilde{\Omega} = -91.08$ and R is increased past bifurcation point at $R = 91.17$ ($l = 2$, $\mu = 0.1$; $K = 4$, $N = 10$).

convergence of the numerical solution is discussed now for a specific example which, however, is typical of all other cases examined. Figure 3(*a*) shows the effect of varying N on the disturbance energy for the same set of parameters as in figure 2(*a*) and fixed $K = 4$. The results strongly suggest that convergence has been achieved to a very good approximation for $N \geqslant 10$. We also note that, using the linear stability of non-rotating pipe flow as a test case, $N = 10$ (which amounts to $2N + 3 = 23$ radial modes) is adequate to reproduce the first few eigenvalues (Salwen, Cotton & Grosch 1980) for $\tilde{R} \leqslant O(10^4)$ and for both 'wall' and 'centre' modes. Thus, there is good reason to believe that convergence of the spectral expansion in the radial direction is satisfactory. On the other hand, figure 3(*b*) shows the effect of increasing K in the same bifurcation diagram as in figure 3(*a*) and fixed $N = 10$. As expected, the

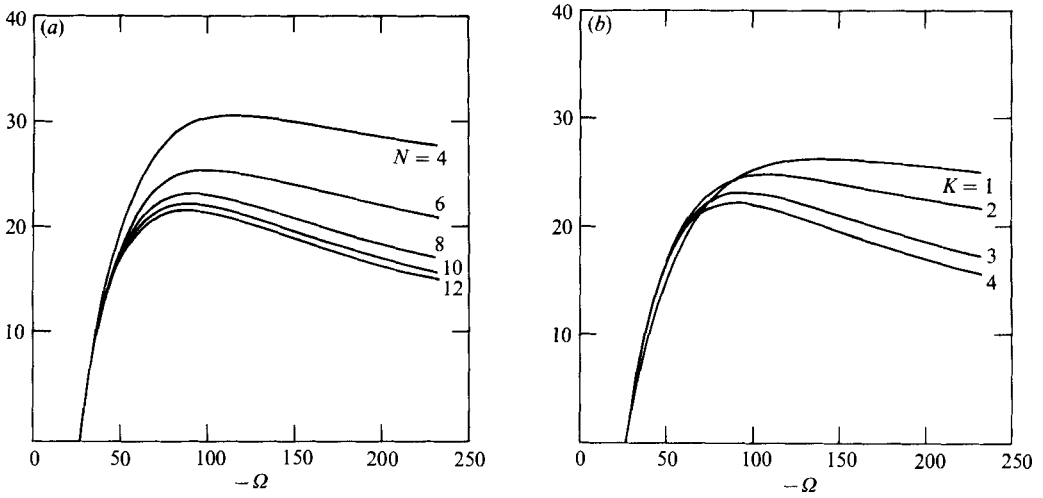

FIGURE 3. Convergence study of the spectral method; disturbance energy $E \times 10^3$ for fixed $\tilde{R} = 106.6$. Ω is increased past bifurcation point at $\Omega = -26.96$ ($l = 1, \mu = 0$). (*a*) Convergence in the number of radial modes N ($K = 4$). (*b*) Convergence in the number of Fourier modes K ($N = 10$).

number of Fourier modes kept is not crucial for very small values of the disturbance energy, close to the bifurcation point, but as the energy increases, there is noticeable variation with K. On the basis of figure 3(*b*), we may conclude that, for the maximum value of $K = 4$ used here, the numerical solution has converged to a good approximation for $|\Omega|$ less than about 70, while for higher rotation, the results are at most qualitatively correct. This rather slow convergence of the Fourier series when the disturbance energy is finite was also noted by Herbert (1977) in plane Poiseuille flow. It is worth emphasizing that, apart from making the computations significantly more expensive, increasing the number of Fourier modes requires calculating (and programming) further nonlinear coupling terms N_m^k in (20), the complexity of which increases dramatically as K is increased. This is a drawback of Galerkin-type methods in general and, thus, if it is necessary to include a large number of Fourier modes, it may be advantageous to calculate the nonlinear terms using a different method (Milinazzo & Saffman 1985). The results shown in figure 1(*a*, *b*) were computed with $K = 2$, $N = 8$ whereas those in figure 2(*a*, *b*, *c*) with the higher resolution $K = 4$, $N = 10$.

All numerical computations were performed on a VAX 11/780 computer using double-precision arithmetic. To increase the efficiency of the program, the nonlinear terms N_m^k were expressed as products of the unknowns a_n^k with known coupling matrices which were pre-calculated and stored (Toplosky 1987). For $K = 4$, $N = 12$, the storage requirements are on the order of 10^6 single-precision words; calculation of the coupling matrices takes about 12 hours and each Newton iteration about 10 min of CPU time. For $K = 4$, $N = 10$ the corresponding CPU times are approximately cut in half.

5. Discussion

Based on the results of the present work, it is clear now that there is no immediate connection between nonlinear spiral waves in slowly rotating pipe flow and possible nonlinear neutral states in non-rotating pipe flow; finite-amplitude spiral waves

bifurcate supercritically from the linear-neutral-stability curve of slowly rotating pipe flow, and there is no sign (at least in the range of parameters that we examined) that the bifurcation branches fold back towards $\Omega = 0$. Supercritical instability of slowly rotating pipe flow could have been inferred from weakly nonlinear theory but, unfortunately, the values of the Landau constant calculated by Akylas & Demurger (1984) were incorrect, suggesting subcritical instability. Thus, the speculation of Akylas & Demurger (1984) is not justified. This certainly does not imply that the nonlinear states of Smith & Bodonyi (1982) do not exist; they were found through an asymptotic analysis, valid as $\tilde{R} \to \infty$, whereas our computations of nonlinear waves were restricted to finite $\tilde{R} \leqslant 500$; furthermore, even in the limit $\tilde{R} \to \infty$, there is no guarantee that these two classes of nonlinear states are connected. In the range $\tilde{R} \leqslant 500$, our computations indicate that the states of Smith & Bodonyi (1982) (if they exist at such values of $\tilde{R}$) cannot be reached by continuation from slowly rotating pipe flow. Also, as $\tilde{R}$ increases, figure 1(*a*) shows that bifurcation of nonlinear spiral waves in slowly rotating pipe flow becomes more supercritical (the real part of the Landau constant remains negative and increases in absolute value); this suggests that, contrary to our original hope, the states of Smith & Bodonyi (1982) most likely lie 'far' from the linear-neutral-stability curve of slowly rotating pipe flow. In such a case, as already discussed in §4, the maximum number of Fourier modes used in the present work ($K = 4$) is inadequate so that any numerical results would probably be of dubious validity. At any rate, our attempt to reach the asymptotic nonlinear states of Smith & Bodonyi (1982) failed, as spiral-wave disturbances in slowly rotating pipe flow do not appear to be directly connected with nonlinear states in non-rotating pipe flow for $\tilde{R}$ finite. Heuristically speaking, it seems that the stability properties of slowly rotating pipe flow are quite different from those of non-rotating pipe flow both for infinitesimal and finite-amplitude perturbations. It is hoped that a careful experiment would be able to identify such a striking difference in the behaviour of these two seemingly almost identical flows.

An interesting feature of finite-amplitude spiral waves in rotating pipe flow, assuming that the axial pressure gradient is held fixed, is the significant mass flux defect, induced by the perturbation Reynolds stresses. Axial mean-flow distortion is relatively more pronounced in the rapid-rotation regime; for the range of parameters examined, in certain cases it can exceed a defect of 45 % of the undisturbed mass flux, while, under the same conditions, the associated relative azimuthal-flow distortion is very small. This can be understood using simple scaling arguments: the linear asymptotic analysis of Pedley (1969) shows that, in the rapid-rotation regime (3), all three perturbation velocity components scale with the basic azimuthal velocity at the pipe wall, ωr_0, which is large compared with the centreline velocity

$$W_0/\omega r_0 = O(\mu).$$

Thus, in the limit $\mu \to 0$, the induced axial mean flow (normalized with the basic axial flow) is expected to be relatively large compared with the induced azimuthal mean flow (normalized with the basic azimuthal flow). Indeed, as shown in figure 2(*b*, *c*), close to the bifurcation point, the induced flux Φ increases much more steeply than the induced circulation Γ. Of course, this qualitative argument cannot reveal that the induced axial mean flow represents a substantial flux defect, a finding that may have some relevance to the phenomenon of vortex breakdown. As already indicated, Ludwieg (1962, 1965) and Pedley (1969) noted that linear spiral instability waves in rotating pipe flow, as they twist in the opposite direction to the swirl of the basic flow

($\Omega < 0$ for $l > 0$), are reminiscent of similar wave disturbances often observed in vortex breakdown. Our calculations of nonlinear spiral waves, and in particular the substantial flux defect found, lend support to this proposal: the spiral waves observed in vortex breakdown are in fact accompanied with axial-flow stagnation (Hall 1972; Leibovich 1978), a phenomenon that cannot be explained in terms of a linear instability mechanism. Nevertheless, it should be emphasized that this analogy between finite-amplitude, strictly periodic spiral waves in rotating pipe flow and unsteady, spatially and temporally evolving, spiral-wave disturbances in vortex breakdown, still remains rather loose; further work is necessary in order to establish a possible connection more precisely.

The authors would like to thank Professor A. T. Patera and Dr S. J. Cowley for valuable discussions on this topic. This work was supported by the National Science Foundation under Grant MSM-8451154. Also, N. Toplosky thanks the Naval Underwater Systems Center for its generous support.

Appendix. Azimuthal wall shear stress

It is clear that, for undisturbed rigidly rotating pipe flow, the azimuthal wall shear stress vanishes and, therefore, no external torque is required to maintain the constant angular velocity of the pipe. Here it is shown that this remains true in the presence of a finite-amplitude spiral-wave perturbation.

In dimensionless variables, the perturbation azimuthal wall shear stress τ is given by

$$\tau = \frac{1}{2\tilde{R}}\left(r\frac{\partial}{\partial r}\frac{v}{r} + \frac{1}{r}\frac{\partial u}{\partial \theta}\right) \quad (r = 1); \tag{A 1}$$

averaging over θ and taking into account the no-slip condition at the pipe wall (A 1) reduces to

$$\tau = \frac{1}{2\tilde{R}}\frac{\mathrm{d}v^0}{\mathrm{d}r} \quad (r = 1). \tag{A 2}$$

Thus, it suffices to show that

$$\frac{\mathrm{d}v^0}{\mathrm{d}r} = 0 \quad (r = 1). \tag{A 3}$$

To this end, consider the azimuthal component of the momentum equation (5) for the $k = 0$ harmonic of the spiral wave (11):

$$\frac{\mathrm{d}^2 v^0}{\mathrm{d}r^2} + \frac{1}{r}\frac{\mathrm{d}v^0}{\mathrm{d}r} - \frac{v^0}{r^2} = \tilde{R}Q, \tag{A 4}$$

where

$$Q = \sum_{k=1}^{\infty}\left[u^k\frac{\mathrm{d}v^{k*}}{\mathrm{d}r} + \mathrm{i}kw^{k*}v^k + \frac{u^{k*}v^k}{r}\right] + *. \tag{A 5}$$

It proves convenient to work with transformed Fourier-component variables:

$$\hat{u}^k = ru^k, \quad \hat{v}^k = rv^k, \quad \hat{w}^k = rw^k, \tag{A 6}$$

so that (A 4) becomes

$$\frac{\mathrm{d}^2\hat{v}^0}{\mathrm{d}r^2} - \frac{1}{r}\frac{\mathrm{d}\hat{v}^0}{\mathrm{d}r} = \tilde{R}\hat{Q}, \tag{A 7}$$

where

$$\hat{Q} = \frac{1}{r}\sum_{k=1}^{\infty}\left[\hat{u}^k\frac{\mathrm{d}\hat{v}^{k*}}{\mathrm{d}r} + \mathrm{i}k\hat{w}^{k*}\hat{v}^k\right] + *. \tag{A 8}$$

Now, multiplying both sides of (A 7) by r, integrating across the pipe radius, and after integration by parts making use of continuity and the no-slip condition, it is finally found that

$$\frac{\mathrm{d}\hat{v}^0}{\mathrm{d}r} = 0 \quad (r = 1), \tag{A 9}$$

which is entirely equivalent to (A 3). This same result can be also obtained directly by an argument based on angular momentum balance. Since the mean flow induced by a spiral wave of permanent form depends on r only, the associated angular momentum remains constant inside a control volume consisting of a pipe section of fixed length. Therefore, the corresponding mean torque has to vanish.

REFERENCES

Abramowitz, M. & Stegun, I. E. 1968. *Handbook of Mathematical Functions*, Dover.

Akylas, T. R. & Demurger, J.-P. 1984 The effect of rigid rotation on the finite-amplitude stability of pipe flow at high Reynolds number. *J. Fluid Mech.* **148**, 193.

Cotton, F. W. & Salwen, H. 1981 Linear stability of rotating Hagen–Poiseuille flow. *J. Fluid Mech.* **108**, 101.

Cowley, S. J. & Smith, F. T. 1985 On the stability of Poiseuille–Couette flow: a bifurcation from infinity. *J. Fluid Mech.* **156**, 85.

Davey, A. 1978*a* On Itoh's finite-amplitude stability theory for pipe flow. *J. Fluid Mech.* **86**, 695.

Davey, A. 1978*b* On the stability of flow in an elliptical pipe which is nearly circular. *J. Fluid Mech.* **87**, 233.

Davey, A. & Nguyen, H. P. F. 1971 Finite-amplitude stability of pipe flow. *J. Fluid Mech.* **45**, 701.

Fox, J. A., Lessen, M. & Bhat, W. V. 1968 Experimental investigation of the stability of Hagen–Poiseuille flow. *Phys. Fluids* **11**, 1.

Hall, M. G. 1972 Vortex breakdown. *Ann Rev. Fluid Mech.* **4**, 195.

Herbert, T. 1976 Periodic secondary motions in a plane channel. in *Proc. 5th Intl Conf. on Numerical Methods in Fluid Dynamics* (ed. A. I. Van de Vooren & P. J. Zandbergen) *Lecture Notes in Physics*, vol. 59, p. 235. Springer.

Herbert, T. 1977 Finite-amplitude stability of plane parallel flows. In *Laminar–Turbulent Transition, AGARD Conf. Proc.* 244, 3–1.

Itoh, N. 1977 Nonlinear stability of parallel flows with subcritical Reynolds numbers. *J. Fluid Mech.* **82**, 469.

Leibovich, S. 1978 The structure of vortex breakdown. *Ann Rev. Fluid Mech.* **10**, 221.

Leite, R. J. 1959 An experimental investigation of the stability of Poiseuille flow. *J. Fluid Mech.* **5**, 81.

Leonard, A. & Wray, A. 1982 A new numerical method for the simulation of three-dimensional flow in a pipe. In *Proc. 8th Intl Conf. on Numerical Methods in Fluid Dynamics* (ed. E. Krause). Springer.

Ludwieg, H. 1962 Zur Erklarung der Instabilitat der uber angestellten Deltaflugeln auftretenden freien Wirbelkerne. *Z. Flugwiss.* **10**, 242.

Ludwieg, H. 1965 Erklarung des Wirbelaufplatzens mit Hilfe der Stabilitatstheorie fur Stromungen mit schraubenlinienformigen Stromlinien. *Z. Flugwiss.* **13**, 437.

Mackrodt, P. A. 1976 Stability of Hagen–Poiseuille flow with superimposed rigid rotation. *J. Fluid Mech.* **73**, 153.

Milinazzo, F. A. & Saffman, P. G. 1985 Finite-amplitude steady waves in plane viscous shear flows. *J. Fluid Mech.* **160**, 281.

Nagib, H. M., Lavan, Z., Fejer, A. A. & Wolf, L. 1971 Stability of pipe flow with superposed solid body rotation. *Phys. Fluids* **14**, 766.

PATERA, A. T. & ORSZAG, S. A. 1981 Finite-amplitude stability of axisymmetric pipe flow *J. Fluid Mech.* **112**, 467.

PEDLEY, T. J. 1969 On the stability of viscous flow in a rapidly rotating pipe. *J. Fluid Mech.* **35**, 97.

SALWEN, H., COTTON, F. W. & GROSCH, C. C. 1980 Linear stability of Poiseuille flow in a circular pipe. *J Fluid Mech.* **98**, 273.

SMITH, F. T. & BODONYI, R. J. 1982 Amplitude-dependent neutral modes in the Hagen–Poiseuille flow through a circular pipe. *Proc. R. Soc. Lond. A* **384**, 463.

TOPLOSKY, N. 1987 Finite-amplitude spiral waves in rotating pipe flow. Ph.D. dissertation, Department of Mechanical Engineering, MIT, Cambridge, MA.

ZAHN, J.-P., TOOMRE, J., SPIEGEL, E. A. & GOUGH, D. O. 1974 Nonlinear cellular motions in Poiseuille channel flow. *J. Fluid Mech.* **62**, 319.